Plant Physiol. (1989) 89, 963–969
0032-0889/89/89/0963/07/$01.00/0

Received for publication July 20, 1988
and in revised form October 17, 1988

Compartmentation of Nucleotides in Corn Root Tips Studied by ^{31}P-NMR and HPLC[1]

Mark A. Hooks, Robert A. Clark, Richard H. Nieman, and Justin K. M. Roberts*

Department of Biochemistry, University of California, Riverside, California 92521 (M.A.H., J.K.M.R.), *and United States Salinity Laboratory, 4500 Glenwood Drive, Riverside, California 92501* (R.A.C., R.H.N.)

ABSTRACT

Corn (*Zea mays* L.) root tips were subjected to different conditions so that nucleotide levels varied over a wide range. Levels of nucleotides in corn root tips were measured using ^{31}P nuclear magnetic resonance (NMR) spectroscopy and high performance liquid chromatography. Results indicate: (a) Similar amounts of NTP and sugar nucleotides were observed by *in vivo* NMR and in extracts. In contrast, a significant amount of NDP observed in root tip extracts was not detected by *in vivo* NMR. Thus, for a given sample, [NTP]/[NDP] ratios determined *in vivo* by ^{31}P-NMR are always higher than ratios observed in extracts, deviating by ~4-fold at the highest ratios. The NMR-invisible pool of NDP appeared quite metabolically inert, barely changing in size as total cell NDP changed. We conclude that NDP in corn root tips is compartmented with respect to NMR visibility, and that it is the NMR-visible pool which responds dynamically to metabolic state. The NMR-invisible NDP could either be immobilized (and so have broad, undetectable NMR signals), or be complexed with species that cause the chemical shift of NDP to change (so it does not contribute to the NMR signal of free NDP), or both. (b) ^{31}P-NMR cannot distinguish between bases (A, U, C, and G) of nucleotides. HPLC analysis of root tip extracts showed that the relative amount of each base in the NTP and NDP pools was quite constant in the different samples. (c) In extracts, for each of the nonadenylate nucleotides, [NTP]/[NDP] was linearly proportional to [ATP]/[ADP], indicating near equilibrium in the nucleoside diphosphokinase (NDPK) reaction. However, the apparent equilibrium constants for the phosphorylation of GDP and UDP by ATP were significantly lower than 1, the true equilibrium constant for the NDPK reaction. Thus, for a given sample, [ATP]/[ADP] ~ [CTP]/[CDP] > [UTP]/[UDP] > [GTP]/[GDP]. This result suggests that the different NDPs in corn root tips do not have equal access to NDPK.

NTP metabolism in plants has been most widely studied by enzymatic or chromatographic analysis of extracts, with attention almost exclusively focused on adenylates (17). More recently, ^{31}P-NMR has been used to examine nucleotide metabolism in living plants (19, 20) and has generated one result potentially in conflict with extract studies: the [NTP]/[NDP] ratios in corn root tips observed *in vivo* by ^{31}P-NMR (22) are significantly higher than [ATP]/[ADP] ratios determined in extracts (25, 26). This apparent discrepancy could result from any, or some combination, of four phenomena, which we address in this study. First, workers using *in vivo* NMR could simply have studied tissues in a different metabolic state than the tissues used in the extract studies; we examined this possibility by directly comparing root tip samples *in vivo* with extracts of the same samples. Second, contributions from nonadenylate nucleotides, which cannot be distinguished from ATP and ADP by ^{31}P-NMR, could in principle make [NTP]/[NDP] > [ATP]/[ADP]; we therefore determined [ATP]/[ADP], [UTP]/[UDP], [CTP]/[CDP] and [GTP]/[GDP] in root tips extracts by HPLC. Third, breakdown of NTP to NDP during extraction would lead to lower [NTP]/[NDP] in extracts than *in vivo*; we tested this possibility by quantitation of NTP and NDP *in vivo* and in extracts. Finally, a significant proportion of certain nucleotides may be undetectable by *in vivo* ^{31}P-NMR due to molecular interactions (*e.g.* with proteins). This could result either from interactions causing immobility, since high resolution NMR detects signals only from freely mobile species (21), or from interactions that cause large changes in chemical shifts, relative to free nucleotides, as occurs on binding of GDP to elongation factor Tu (31). Any such distinctions between nucleotides *in vivo* is lost on extraction. Compartmentation of nucleotides between immobilized and freely mobile pools was suggested in NMR studies of human blood platelets (4, 28), skeletal muscle (7), and rat kidney (6), from comparison of the amounts of nucleotides visible *in vivo* and in extracts. Such comparisons were made in this study, and our results indicate the existence of an NMR-invisible pool of NDP *in vivo*.

Compartmentation of nucleotides in cells can also be inferred from metabolite analysis of near-equilibrium reactions. The mass action ratio for a reaction known to operate near equilibrium *in vivo* is determined by analysis of the whole cell or tissue. Compartmentation of one or more substrates away from the particular enzyme is suggested when the mass action ratio differs significantly from the equilibrium constant. Using this approach, together with a comparison of tissues differing in mitochondrial content, Veech *et al.* (29) concluded that much of the ADP in cells is sequestered in mitochondria, and therefore inaccessible to cytoplasmic enzymes on the timescale of nucleotide turnover (seconds). Here we described an analogous study of the NDPK[2] reaction, using HPLC to analyze root tip extracts. NDPK catalyzes the transfer of the

[1] Supported by National Science Foundations grants DMB 8521564 and DMB 8604091; U.S. Department of Energy grant FG03-86ER13535; and National Institutes of Health (PHS BRSG 2 507).

[2] Abbreviations: NDPK, nucleoside diphosphokinase; MDP, methylene diphosphonate; cNADP, β-NAD-2′:3′-cyclic monophosphate.

terminal phosphate from NTP to NDP (14). *In vivo*, ATP produced via oxidative phosphorylation normally drives phosphorylation of NDPs produced by metabolism (18). The equilibrium constant of the NDPK reaction is approximately 1 (14). The activity of NDPK in many tissues is high relative to activities of other enzymes (1, 14), such that near equilibrium is anticipated (18). Our analysis suggests compartmentation of the different NDPs in corn root tips with respect to access to NDPK.

MATERIALS AND METHODS

Plant Material

Corn (*Zea mays* L.) hybrid Funk 4323 (Germain's Seeds, Los Angeles, CA) was soaked in water for 24 h, then germinated in the dark for 36 to 48 h. Two g (~1000) 2 mm long root tips were excised on ice with a razor blade, rinsed and transferred to a 3 mL plastic syringe (~10 mm diameter) (the NMR sample tube). A capillary tube containing 0.5 M MDP in Tris (pH 8.9) was placed in the center of the sample tube. The sample was perfused as described previously (19). Perfusion conditions were varied to produce a wide range of NTP/NDP ratios in the different samples analyzed. NTP/NDP ratios in samples perfused rapidly (>15 mL/min) with an oxygen-bubbled solution were consistantly greater than 20, while those for samples perfused slowly (7–8 mL/min) with an air saturated, 100 μM KCN solution were as low as 0.5.

Nucleotide Extraction

After NMR data accumulation, the syringe was drained and the tissue rapidly frozen by immersion in liquid nitrogen. A modified TCA in ether procedure was used for nucleotide extraction (30). This method has been described as the most reliable procedure for nucleotide extraction (15); we found this to be so, compared to extractions using perchloric acid, as we employed previously (22). The frozen sample was removed from the syringe and placed in a −20°C mortar with 60 μL of a frozen solution of 6.9 mM cNADP and 7.0 mM XMP, both from Sigma, St. Louis, MO. The sample was ground to a fine powder at −20°C, then transfered on dry ice to a fume hood. Nine mL of 0.6 M TCA/ether, chilled on dry ice, was added and the sample homogenized for 1 min. The slurry and solid residue were spun at 16,000*g* for 10 min at 4°C in a stainless steel tube with cap. The supernatant was saved and 2 mL TCA/ether added to the pellet, which was resuspended and recentrifuged. The two supernatants were pooled and extracted twice with equal volumes of water. The aqueous phases were pooled and washed four times with two volumes of ether to remove the TCA. The remaining water phase was vigorously bubbled with nitrogen gas to remove the ether. Samples were neutralized with KOH, frozen, and lyophilized. Samples were resuspended in 600 μL of extraction buffer (60 mM Mops, 2 mM EDTA, 15 mM $MgCl_2$, brought to pH 7.6 with Tris base) and transferred to a 5 mm NMR tube containing the MDP capillary reference. The high magnesium ion concentration was used to resolve the signal of the internal standard (cNADP) from the low field sugar nucleotide resonance (see peaks 5 and 6 in Fig. 1E).

NMR Spectroscopy

Fourier transform ^{31}P-NMR spectra were obtained on a General Electric GN500 spectrometer operating at 202.5 MHz. Neither field frequency locking nor proton noise decoupling was used. Chemical shifts are referenced to external MDP, at 0 ppm. All spectra were obtained under nonsaturating conditions (pulse interval 5 s; pulse angle ~60°) so that peak intensity was proportional to concentration in the NMR tube (19). *In vivo* NMR spectra were acquired in 1 h blocks so that the stability of spectra over time could be established. Several blocks were added together to give spectra of sufficient signal/noise for nucleotide quantitation. Typical acquisition times are given in the legend to Figure 1. Spectra of extracts were acquired over ~5 h; no changes in extract spectra were observed over 24 h at room temperature. All NMR spectra peaks were integrated by cutting and weighing. NTP was determined from the area of the γ-NTP resonance, NDP from the β-NDP resonance (Fig. 1) (22). The higher free magnesium concentration in the extracts relative to *in vivo* (~1 mM) (19) resulted in less frequency separation between γNTP and βNDP, and resolution αNTP and αNDP (compare Fig. 1, B and C).

Nucleotides *in vivo* were quantitated by comparing their respective peak areas to the peak area of a 1 mM phosphate solution in a 3 mL syringe. Comparison was made using the signal from MDP (contained in a coaxial glass capillary in both samples) as a reference. This comparison gave nucleotide concentrations in the NMR detection volume. To convert concentrations to content (μmol/500 root tips), this concentration was multiplied first by the volume of 500 root tips (initially ~1.21 mL) and second by the growth factor (final/initial volume). Nucleotides in extracts were quantitated using the signal from the cNADP internal standard (620 nmol ^{31}P/500 root tips). The contribution from endogenous NAD(P) to the cNADP signal was subtracted using a standard curve of NAD(P) peak height *versus* [NTP]/[NDP], determined from spectra of 21 root tip extracts, varying in [NTP]/[NDP], to which cNADP was not added. The area of the endogenous NAD(P) signal was ~20% of the cNADP signal (Fig. 1).

HPLC

After NMR analysis, the extract was purified using the tricolumn system described by Nieman *et al.* (11). HPLC was performed using the following equipment: 2 Altex model 100 pumps controlled by a Altex model 420 microprocessor; Hewlett Packard 1040A HPLC-[diode-array] detection system; Hewlett packard 85B computer and integration system; Rheodyne model 7120 injector with a 20 μL loop; Whatman Partisphere 5 SAX anion exchange cartridge column (250 × 4.6 mm); Whatman guard column of the same material; silica saturator preguard column packed with 50 μm silica gel; Orion Research digital pH meter 611. The separating, guard, and preguard column were held at 30°C with water jackets. The buffer and gradient system were as described previously (12). Peaks were identified based on comparison of retention times and absorption spectra of authentic, pure nucleotide. Nucleotides were quantitated using the XMP internal standard. The ratio of peak areas, nucleotide/XMP, recorded at

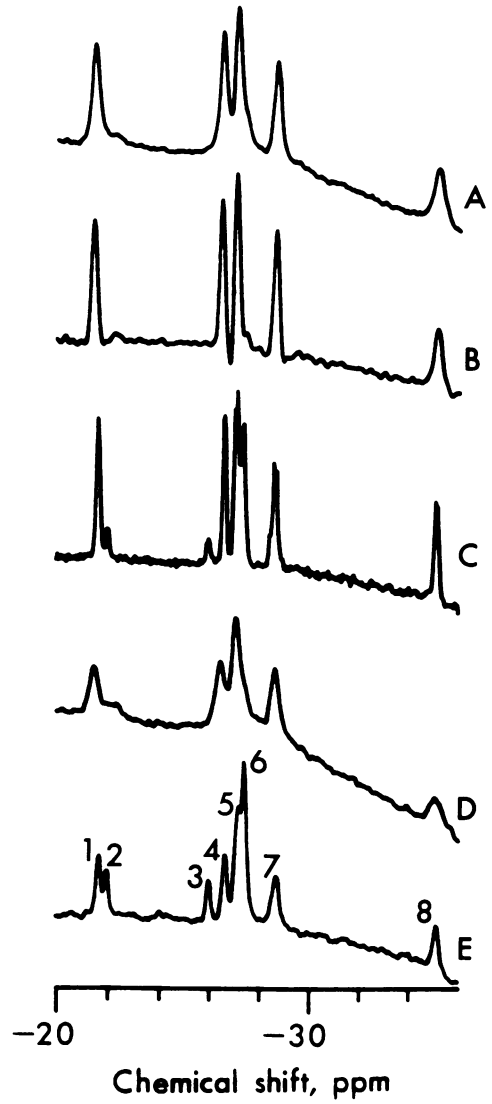

Figure 1. ^{31}P-NMR spectra of nucleotides in perfused corn root tips and corresponding extracts. (A) Root tips perfused in O_2-saturated 0.1 mM $CaSO_4$; flow rate 7 mL/min; 12 h accumulation; 15 Hz line-broadening; [NTP]/[NDP] = 10. (B) Same free induction decay giving spectrum (A), but with double exponential multiplication (5) applied prior to Fourier transformation (DM = 12); [NTP]/[NDP] = 11. (C) Extract of sample giving spectra (A) and (B); 8 h accumulation; 3 Hz line-broadening; [NTP]/[NDP] = 4. (D) Root tips perfused in air-saturated 0.1 mM $CaSO_4$ plus 10 μM KCN, pH 7.5; flow rate 7 mL/min; 5 h accumulation ; [NTP]/[NDP] = 2.5. (E) Extract of sample giving spectrum (D); 10 Hz line-broadening; [NTP]/[NDP] = 1.5. Peak assignments: 1, γ-NTP; 2, β-NDP; 3, α-NDP (resolved only in extract); 4, α-NTP (overlaps with α-NDP in tissue spectra); 5, sugar nucleotides; 6, cNADP (present only in extract); 7, sugar nucleotides; 8, β-NTP.

260 nm was multiplied by the ratio of ϵ_{260S} (XMP/nucleotide), determined at the ionic strength and pH at which the compounds eluted from the column. This value was multiplied by the amount of XMP added to the sample (210 nmol/500 root tips).

RESULTS

Differences between NTP/NDP Ratios Observed *in vivo* and in Extracts Are Due to Pools of NMR-Invisible NDP

When a given corn root tip sample was examined *in vivo* by ^{31}P-NMR, [NTP]/[NDP] was consistently higher than in the corresponding extract (Fig. 2). Further, the highest value of [NTP]/[NDP] (or [ATP]/[ADP] discussed below) in extracts reported here are similar in magnitude to the highest values reported by others (*e.g.* Refs. 25 and 26). Therefore, the differences in [NTP]/[NDP] between *in vivo* ^{31}P-NMR and extract analyses must be due to changes during extraction; either conversion of NTP to NDP, or release of bound and NMR-invisible NDP, such that more NDP is detected in the extract. We distinguished between these two possibilities by determining the absolute amounts of NTP and NDP observed *in vivo* and in extracts by ^{31}P-NMR (Figs. 3 and 4). No difference between the amount of NTP observed *in vivo* and in extracts was apparent (Fig. 3). Hence, breakdown of NTP during extraction was negligible. (Likewise, equivalent amounts of total sugar nucleotides were observed *in vivo* and in extracts [data not shown]). In contrast, the amount of NDP observed *in vivo* was always much lower than that found in extracts (Fig. 4). These results indicate that there is a sizeable pool of NDP in corn root tips that is not detected by *in vivo* NMR. The size of this NMR-invisible pool of NDP, given by the difference between the two data sets in Figure 4, showed little response to the metabolic state of the tissue, appearing quite similar in all samples examined. The increase in detectable NDP that was seen on extraction was similar in samples regardless of the amount of NTP (Figs. 3 and 4), a result consistent with the above conclusion that increased NDP was not due to NTP breakdown.

Proportions of Bases in Nucleotides are Insensitive to Metabolic State

While ^{31}P-NMR can be used to observe nucleotides *in vivo*, it cannot distinguish between nucleotides having different

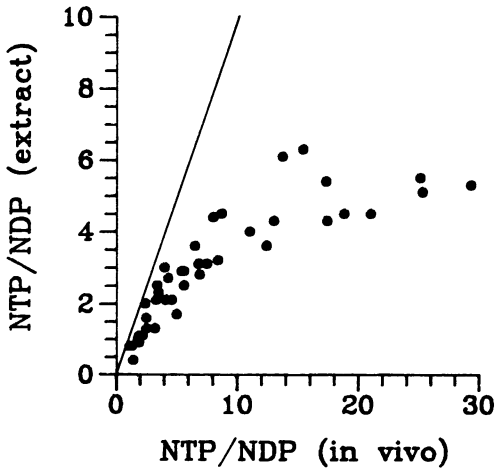

Figure 2. NTP/NDP ratios in corn root tips and corn root tip extracts determined by ^{31}P-NMR. Each point represents one tissue sample from which both *in vivo* and extract ratios were determined. The line shows where values for the two ratios are equal.

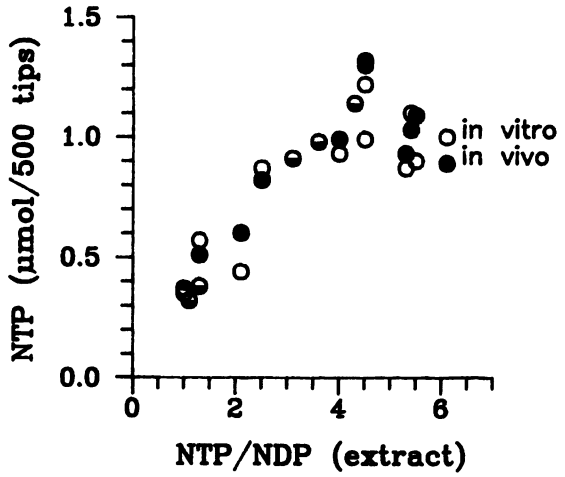

Figure 3. NTP content in corn root tips (●) and the corresponding extracts (○) determined by ^{31}P-NMR. The half-filled circles (◒) denote those samples with the same amounts determined *in vivo* and in extracts. The mean of the [NTP](*in vivo*/[NTP](extract) ratios was 1.03, SD ± 0.16.

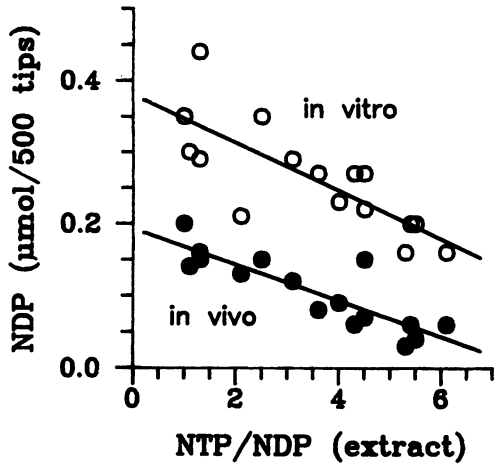

Figure 4. NDP content in corn root tips (●) and the corresponding extracts (○), determined by ^{31}P-NMR.

bases. Hence, we examined root tip extracts by HPLC to determine how the relative amounts of each nucleotide changed with metabolic state. Under the diverse conditions used here, we found little change in the relative amounts of A, U, C, and G in NTPs, NDPs, and sugar nucleotides (Figs. 5–7). The largest change observed was in ATP, which increased from ~45% to ~60% of total NTP, as [NTP]/[NDP] increased.

Evidence for Compartmentation of NDP from Analysis of the NDPK Reaction

We examined the NDPK reaction in corn root tips by HPLC analysis of nucleotides in extracts. For nonadenylates, [NTP]/[NDP] displayed a linear dependence on [ATP]/[ADP] (Fig. 8). Each of the treatments giving lower [NTP]/[NDP] (exposure to KCN and/or low oxygen tension) act specifically at the level of oxidative phosphorylation. Hence,

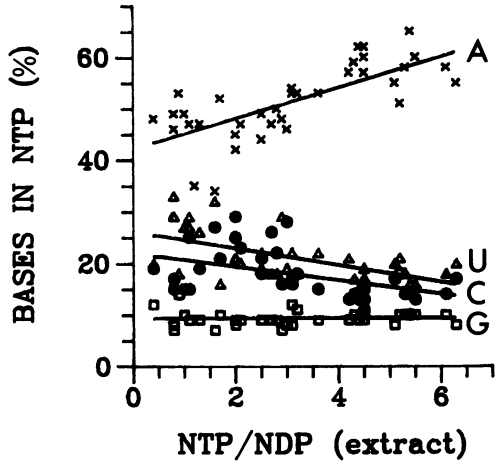

Figure 5. Relative abundance of bases A, U, C, and G in NTP in corn root tip extracts, determined by HPLC.

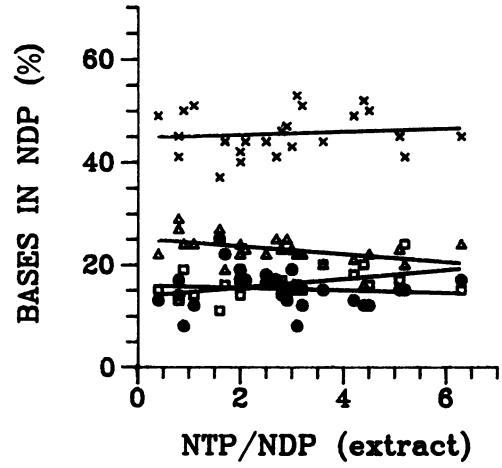

Figure 6. Relative abundance of bases in NDP in corn root tip extracts, determined by HPLC. Symbols as in Figure 5.

they must serve first to decrease [ATP]/[ADP]; decreases in [NTP]/[NDP] of nonadenylates must be a secondary response. The results indicate that the NDPK reaction is near equilibrium. Thus, the behavior of the data in Figure 8 is consistent with Le Châtelier's principle (2): when [ATP]/[ADP] is perturbed, nonadenylates respond in a way such that [NTP][ADP]/[ATP][NDP] is constant. The treatments employed in this study result in the rate of turnover of ATP varying over a ~10-fold range, decreasing as [NTP]/[NDP] decreases (22, 23). If the NDPK reaction was not near equilibrium *in vivo* then, as the rate of production of NDP and ATP decreased, [NTP][ADP]/[ATP][NDP] would tend to the equilibrium constant, since these fluxes would be responsible for any disequilibrium among reactants accessible to NDPK. Such behavior was not observed, suggesting near equilibrium of the NDPK reaction under all conditions.

However, one aspect of the results in Figure 8 is inconsistent with the idea of near-equilibrium of total cellular NTP and NDP via the NDPK reaction. The slopes of the lines for U and G are 0.63 and 0.42, respectively—significantly less than 1, the equilibrium constant for the NDPK reaction (14). (We

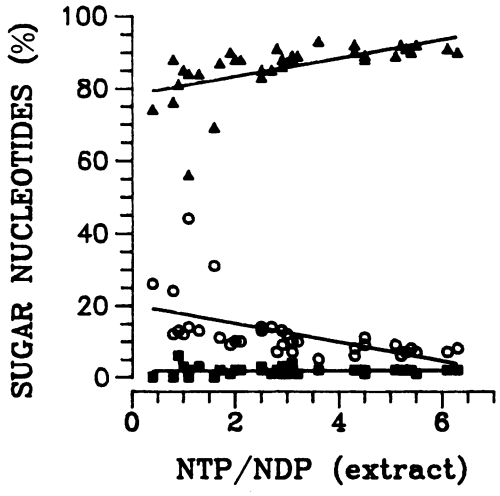

Figure 7. Relative abundance of sugar nucleotides in corn root tip extracts, determined by HPLC. Symbols: (▲), UDP-Glc; (○), UDP-GlcNAc; (■), GDP-Glc. Other sugar nucleotides (*e.g.* ADP-Glc) were not detected (<1% of total).

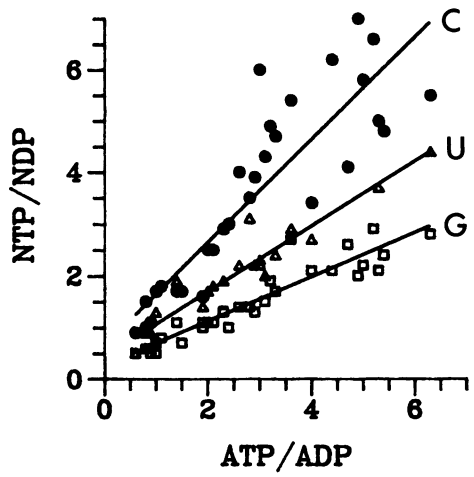

Figure 8. Dependence of [GTP]/[GDP], [UTP]/[UDP] and [CTP]/[CDP] on [ATP]/[ADP] in corn root tip extracts, determined by HPLC. The slope of each line gives the apparent equilibrium constant for the particular NDPK reaction, and are 1.0, 0.63, and 0.42 (with correlation coefficients of 0.88, 0.95, and 0.93; $P < 0.001$) for C, U, and G, respectively.

checked the value of this equilibrium constant by HPLC analysis of mixtures of NTPs and NDPs, incubated in the presence of 3 mM $MgCl_2$, 20 mM KPi, and 5 units/mL NDPK [Sigma] at pH 7.0 for 1 h. In three separate experiments using different initial nucleotide concentrations and ratios, we found mean equilibrium constants (±SD) of 0.83 ± 0.01, 0.98 ± 0.05, and 0.93 ± 0.06 for U, G, and C, respectively.) If the NDPK reaction is near-equilibrium, the non-ideal behavior in Figure 8 suggests the existence of pools of nucleotides sequestered away from NDPK, such that only a portion of the total cellular NDP could be equilibrated via the NDPK reaction. In the latter case, more UDP and, particularly, GDP would be inaccessible to NDPK, relative to other nucleotides, accounting for the fact that total cellular [GTP]/[GDP] < [UTP]/[UDP] < [CTP]/[CDP] ~ [ATP]/[ADP]. This is discussed below with respect to the results of our NMR experiments.

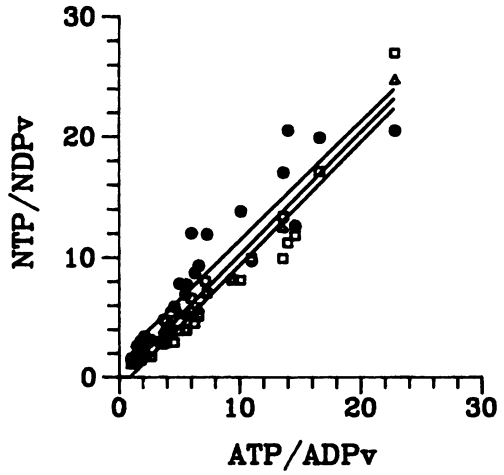

Figure 9. Near-equilibrium in the NDPK reaction for NMR-visible nucleotides in corn root tips. The graph is a theoretical plot of data derived from Figure 8, assuming that NMR-invisible NDP is inaccessible to NDPK, and that this NDP is slightly enriched in GDP and UDP (see "Discussion"), as follows. For each sample in Figure 8 the percent of total cell NDP (NDP_t) that is NMR-invisible (NDP_i) was determined from Figure 4 (this varies with [NTP]/[NDP]). Relative to this value of (NDP_i/NDP_t) × 100, we set the corresponding percentages for GDP_i/GDP_t to be 10% higher; 2% higher for UDP_i/UDP_t; and 8% lower for both ADP_i/ADP_t and CDP_i/CDP_t. This operation simulated enrichment of NDP_i with GDP and UDP. Subtraction of these NMR-invisible NDPs from the total amounts of the four NDPs, determined by HPLC, gave the NMR visible GDP, UDP, etc. From this, the NMR-visible [GTP]/[GDP], [UTP]/[UDP], etc., were calculated. These values are presented here. The slopes of the linear best fit lines are 0.99, 1.02, and 1.02 (with correlation coefficients of 0.93, 0.98 and 0.97; $P < 0.001$) for C, U, and G, respectively. Symbols as in Figure 8.

DISCUSSION

An important practical and long-recognized consequence of compartmentation of nucleotides in cells is that enzymes participating in metabolism can experience nucleotide concentrations and ratios very different from those observed in cell extracts (*e.g.* Ref. 10). The results presented above provide two lines of evidence for compartmentation of nucleotides in corn root tips. First, compartmentation with respect to NMR visibility. The amount of NDP seen *in vivo* is lower than in extracts (Fig. 4). Qualitatively similar results have been reported from NMR studies of human blood platelets (4, 28), skeletal muscle (7), and rat kidney (6), where it was concluded that NMR-invisible nucleotides present *in vivo* were immobilized; immobilized species give broad signals that are undetectable in high resolution experiments. Hence, existence of an immobilized pool of NDP in corn root tips is one possible explanation for the result in Figure 4. Such immobilized nucleotides contrast with nucleotides bound to certain enzymes, which retain significant mobility and therefore are visible by high resolution NMR (for review, see Ref. 24), as are "free" nucleotides. The chemical shifts of nucleotides may

change only slightly on binding to enzymes, as in the case of ATP and arginine kinase (16), or significantly, for example the ~3 ppm shift in the β-GDP resonance on binding to elongation factor Tu from *Escherichia coli* (31). *In vivo*, NDP could be bound to many different proteins, each complex having a different chemical shift, so that the spectrum of such a mixed population of complexes could consist of a broad line. To date, the relative contributions of signals from "free" and enzyme-bound, but still freely mobile, nucleotides to *in vivo* ^{31}P-NMR spectra have not been determined.

Second, we provide evidence for compartmentation of NDP with respect to accessibility to the enzyme NDPK, on the time-scale of nucleotide turnover (seconds). Results of HPLC analysis of extracts indicated near-equilibrium of the NDPK reaction (Fig. 8). However, for root tips in a given metabolic state, nucleotides containing U and, particularly, G were always less phosphorylated than the nucleotides containing A and C. We suggested that this behavior would occur if corn root tips contained a pool of NDP inaccessible to NDPK, this pool being enriched in GDP and UDP. The plausibility of this model can be tested, using the results of our ^{31}P-NMR experiments. We postulate that the pool of NMR-invisible NDP (Fig. 4) is inaccessible to NDPK. This would be likely if the NMR-invisible pool were immobilized, as suggested above. If the contribution from NMR-invisible NDPs (enriched in GDP and UDP) is subtracted from the data given in Figure 8, [NTP]/[NDP] for every nonadenylate exhibits a linear dependence on [ATP]/[ADP], with a slope of ~1, equal to the true equilibrium constant for the NDPK reaction (14) (Fig. 9). While this analysis is consistent with the idea that NMR invisible nucleotides do not have ready access to NDPK, it remains to be shown whether or not this is actually the case.

We can only speculate as to the location of the NMR-invisible NDPs in corn root tips. Mitochondria have been found to contain lower [ATP]/[ADP] than cytoplasm in a wide variety of tissues and organisms (for review, see Refs. 9 and 17). And Veech *et al.* (29) have presented evidence that much of the ADP in animal cells capable of respiration is sequestered in mitochondria, out of equilibrium with cytoplasmic enzymes. Nucleotides in rat liver mitochondria give broad NMR signals compared to signals of *in vivo* spectra (13). Based on these studies we can postulate that some of the NMR-invisible NDP in corn root tips is located in mitochondria. In plant cells, mitochondria generally take up a smaller proportion of the volume than in many animal cells (27). This difference may account for the fact that the amount of NDP that is NMR-invisible in corn root tips (~0.15 μmol/g fresh weight; Fig. 4) is smaller than the NMR-invisible NDP pool in rat kidney (~1 μmol/g fresh weight) (6), a tissue rich in mitochondria. We consider it unlikely, however, that all the NMR-invisible NDP is sequestered in this organelle. For example, NDP bound to proteins such as elongation factor 2 (3) or polymerized tubulin (8), might not contribute to the intensity of the β-NDP signal at ~−22 ppm (Fig. 1), because of either broadening from immobilization, or a change in the chemical shift of β-NDP as occurs when GDP binds to prokaryotic elongation factor Tu (31). The dissociation constant for eukaryotic elongation factor 2:GDP complex (~1 μM) (3) is much smaller than the concentration of GDP in corn root tips (~30 μM). Hence the amount of GDP bound to proteins such as elongation factor 2 will not change as the NDP content changes with metabolic state. Such behavior mirrors that of the NMR-invisible pool in corn root tips, which does not respond to the size of the freely mobile pool (Fig. 4).

If NDP *in vivo* is rendered NMR-invisible by interaction with proteins, one can infer from Figures 4, 6, and 9 that (a) most of the NMR-invisible NDP binds to these proteins with dissociation constants much lower than the lowest concentration of NMR-visible NDP *in vivo* (~10^{-5} M); (b) the concentration of NDP-binding sites having dissociation constants < ~10^{-4} M is ~0.15 μmol/500 root tips, the concentration of NMR-invisible NDP; and (c) the proportion of UDP and, particularly, GDP bound to these sites is higher than in the total NDP pool. It should be possible to test for the existence of such strong nucleotide-binding proteins in cell extracts (*cf.* for example, Ref. 8). The effect of these nucleotide-binding sites, and others that bind nucleotides less tightly, on the concentrations and ratios of free nucleotides in cells remains to be determined.

LITERATURE CITED

1. **Abdul-Baki AA, Ray PM** (1971) Regulation by auxin of carbohydrate metabolism involved in cell wall synthesis by pea stem tissue. Plant Physiol **47:** 537–544
2. **Atkins PW** (1978) Physical Chemistry, Ed 2. Oxford University Press, Oxford, p 269
3. **Bermek E, Nurten R, Bilgin-Aktar N, Odabas UG, Sayhan OZ** (1985) Guanine nucleotide binding to eukaryotic elongation factor 2: a possible control mechanism of eukaryotic chain elongation. *In* E Bermek, ed, Mechanisms of Protein Synthesis. Springer, New York, pp 180–191
4. **Costa JL, Dobson CM, Kirk KL, Poulsen FM, Valeri CR, Vecchione JJ** (1979) Studies of human platelets by ^{19}F and ^{31}P NMR. FEBS Lett **99:** 141–146
5. **Ferrige AG, Lindon JE** (1978) Resolution enhancement in FT NMR through the use of a double exponential function. J Magn Reson **31:** 337–340
6. **Freeman D, Bartlett S, Radda G, Ross B** (1983) Energetics of sodium transport in the kidney. Saturation transfer ^{31}P-NMR. Biochim Biophys Acta **762:** 325–336
7. **Gadian DG** (1982) Nuclear Magnetic Resonance and Its Application to Living Systems. Oxford University Press, Oxford
8. **Jacobs M, Smith H, Taylor EW** (1974) Tubulin: nucleotide binding and enzymic activity. J Mol Biol **89:** 455–468
9. **Klingenberg K, Heldt HW** (1982) The ADP/ATP translocator in mitochondria and its role in intracellular compartmentation. *In* H Sies, ed, Metabolic Compartmentation. Academic Press, New York, pp 101–122
10. **Krebs HA** (1973) Pyridine nucleotides and rate control. Symp Soc Exp Biol **27:** 299–318
11. **Nieman RH, Pap RH, Clark RA** (1978) Rapid purification of plant nucleotide extracts with XAD-2, polyvinylpolypyrrolidone, and charcoal. J Chromatogr **161:** 137–146
12. **Nieman RH, Clark RA** (1984) Measurement of plant nucleotides by high-performance liquid chromatography. J Chromatogr **317:** 271–281
13. **Ogawa S, Lee T-M** (1982) Proton stoichiometry of adenosine 5′-triphosphate synthesis in rat liver mitochondria studied by phosphorus-31 nuclear magnetic resonance. Biochemistry **21:** 4467–4473
14. **Parks RE, Agarwal RP** (1973) Nucleoside diphosphokinases. *In* PD Boyer, ed, The Enzymes, 3, Vol 8. Academic Press, New York, pp 307–333

15. **Pradet A, Raymond P** (1983) Adenine nucleotide ratios and adenylate energy charge in energy metabolism. Annu Rev Plant Physiol **34:** 199–224
16. **Rao BDN, Cohn M** (1977) ^{31}P nuclear magnetic resonance of bound substrates of arginine kinase reaction. J Biol Chem **252:** 3344–3350
17. **Raymond P, Gidrol X, Salon C, Pradet A** (1987) Control involving adenine and pyridine nucleotides. *In* DD Davies, ed, The Biochemistry of Plants, Vol 11. Academic Press, New York, pp 129–176
18. **Reich JG, Sel'Kov EE** (1981) Energy Metabolism of the Cell. Academic Press, New York
19. **Roberts JKM** (1986) Determination of the energy status of plant cells by ^{31}P-nuclear magnetic resonance. *In* HF Linskens, JF Jackson, eds, Modern Methods of Plant Analysis, Vol 2. Springer, New York, pp 43–59
20. **Roberts JKM** (1987) NMR in plant biochemistry. *In* DD Davies, ed, The Biochemistry of Plants, Vol 13. Academic Press, New York, pp 181–227
21. **Roberts JKM, Jardetzky O** (1985) NMR in biochemistry. *In* AM Neuberger, LLM van Deenan, eds, Modern Physical Methods in Biochemistry. Elsevier, Amsterdam, pp 1–67
22. **Roberts JKM, Lane AN, Clark RA, Nieman RH** (1985) Relationships between the rate of synthesis of ATP and the concentrations of reactant and products of ATP hydrolysis in maize root tips, determined by ^{31}P nuclear magnetic resonance. Arch Biochem Biophys **240:** 712–722
23. **Roberts JKM, Wemmer D, Jardetzky O** (1984) Measurement of mitochondrial ATPase activity in maize root tips by saturation transfer ^{31}P nuclear magnetic resonance. Plant Physiol **74:** 632–639
24. **Rösch P** (1986) NMR-studies of phosphoryl transferring enzymes. Prog NMR Spectrosc **18:** 123–169
25. **Saglio PH, Raymond P, Pradet A** (1980) Metabolic activity and energy charge of excised maize root tips under anoxia. Plant Physiol **66:** 1053–1057
26. **Saglio PH, Drew MC, Pradet A** (1988) Metabolic acclimation to anoxia induced by low (2–4 kP_a partial pressure) oxygen pretreatment (hypoxia) in root tips of *Zea mays*. Plant Physiol **86:** 61–66
27. **Steer MW** (1981) Understanding Cell Structure. Cambridge University Press, Cambridge
28. **Ugurbil K, Holmsen H, Shulman RG** (1979) Adenine nucleotide storage and secretion in platelets as studied by ^{31}P nuclear magnetic resonance. Proc Natl Acad Sci USA **76:** 2227–2231
29. **Veech RL, Lawson JWR, Cornell NW, Krebs HA** (1979) Cytosolic phosphorylation potential. J Biol Chem **254:** 6538–6547
30. **Wilson AM, Harris GA** (1966) Hexose-, inositol-, and nucleoside phosphate esters in germinating seeds of crested wheatgrass. Plant Physiol **41:** 1416–1419
31. **Wittinghofer A, Goody RS, Roesch P, Kalbitzer HR** (1982) The structure of the EF-Tu·GDP·Me^{2+} complex. Eur J Biochem **124:** 109–115